6th International Symposium on Hydraulic Structures Portland, Oregon, USA, 27-30 June 2016
Hydraulic Structures and Water System Management
ISBN 978-1-884575-75-4 DOI: 10.15142/T3670628160853

Free-Surface Aeration in a Steep Stepped Spillway

G. Zhang[1] and H. Chanson[1]
[1]Dept. of Civil Engineering
The University of Queensland
St Lucia, QLD 4072
Australia
E-mail: h.chanson@uq.edu.au

ABSTRACT

Self-aeration has important civil and environmental applications in stepped chutes, ranging from cavitation protection to enhanced air-water mass transfer. Air bubble entrainment occurs when the turbulent stresses in the boundary layer exceed the combined effects of surface tension and buoyancy. The governing equations for air diffusion in the rapidly-varied region next to and in the gradually-varied region away from the inception point of aeration are introduced. New and existing solutions to these equations are discussed and compared with new experimental data. An analytical model for flow bulking is introduced. The concept of negative diffusivity is discussed.

Keywords: *Free-surface aeration, stepped spillways, inception point, rapidly varied flow, physical modelling, turbulent mixing.*

1. INTRODUCTION

Self-aeration on stepped chutes occurs once the turbulent stresses in the turbulent boundary layer exceed the combined effects of surface tension and buoyancy (Rao and Rajaratnam 1961, Ervine and Falvey 1987, Chanson 1993, 2008). This location is known as the inception point of free-surface aeration (Wood et al. 1983, Chanson 1994), where the depth averaged void fraction is about 0.2 (Matos 2000). The flow undergoes some rapid bulking immediately downstream of the inception point, after which some de-aeration might occur (Matos 1999). On a relatively long chute, the flow eventually becomes gradually-varied and tends to a pseudo-equilibrium.

This paper presents a comprehensive analysis of the air diffusion process downstream of the inception point. A new model is proposed to describe flow bulking in the rapidly varied flow region and is compared with experimental results. The concept of negative diffusivity is introduced and is shown to be linked with flow de-aeration.

2. EXPERIMENTAL FACILITY AND INSTRUMENTATION

New experiments were conducted in a large-size stepped spillway model (1V:1H) at the University of Queensland (UQ). The chute consisted of 12 steps made of smooth painted marine ply, each step being 0.1 m long, 0.1 m high, and 0.985 m wide. The chute inflow was controlled by a 1.2 m high broad crested weir with a crest size of 0.6 m × 0.985 m (length × width). The weir crest was rounded at both upstream (0.058 m radius) and downstream (0.012 m radius) edges to ensure a smooth inflow. The experimental facility is sketched in Figure 1. Air-water measurements were conducted with a dual-tip phase detection probe at and between step edges downstream of the inception point. Each tip consisted of an inner and an outer electrode respectively made of silver (0.25 mm diameter) and stainless steel (0.8 mm diameter). Data were sampled at 20 kHz per sensor for 45 s. The probe was mounted along the channel centerline with vertical adjustment controlled by a Mitutoyo™ digital scale with an accuracy of ±0.01 mm.

Detailed air-water flow measurements were performed in the mainstream flow above the pseudo-bottom at every step edge downstream of the inception point. Additional measurements were performed between step edges in the mainstream flow and inside the step cavities. The mainstream and cavity air-water flow measurements were respectively performed with the probe sensor aligned parallel to the pseudo-bottom and to the horizontal step face,

as sketched in Figure 2. All measurements were conducted on the channel centerline. The experimental flow conditions focused on skimming flows corresponding to Reynolds numbers between 3.4×10^5 – 8.8×10^5 and are summarized in Table 1.

Table 1. Summary of experimental flow conditions

d_c/h	Q (m^3/s)	Location	Inception Point	Re
0.9	0.083	step edges 5-12 step cavities: 7-8, 8-9	step edge 5	3.3×10^5
1.1	0.112	step edges: 5-12 step cavities: 7-8, 8-9	step edge 5	4.6×10^5
1.3	0.145	step edges: 7-12 step cavities: 7-8, 8-9	step edge 7	5.9×10^5
1.5	0.179	step edges: 7-12 step cavities: 10-11, 11-12	step edge 7	7.3×10^5
1.7	0.216	step edges: 9-12	step edge 9	8.8×10^5

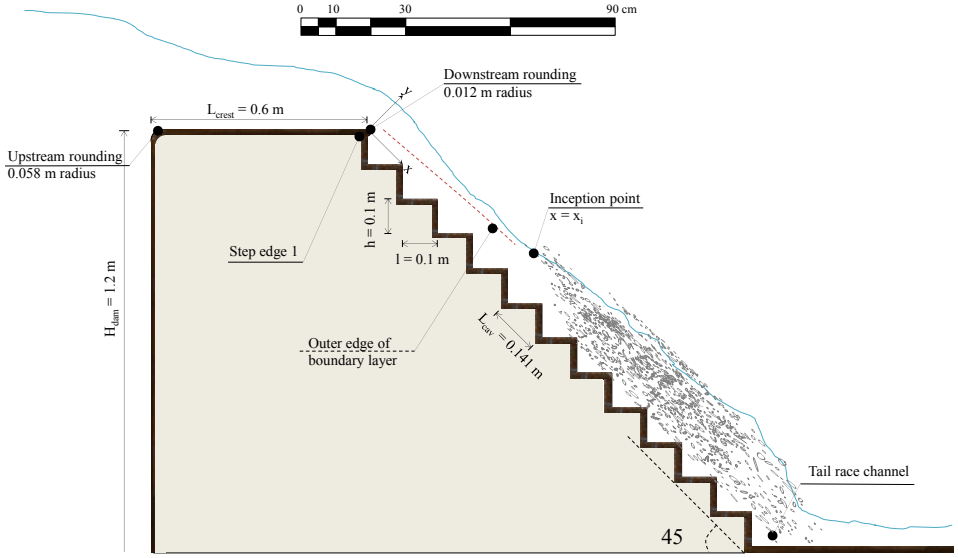

Figure 1. Sketch of the experimental facility.

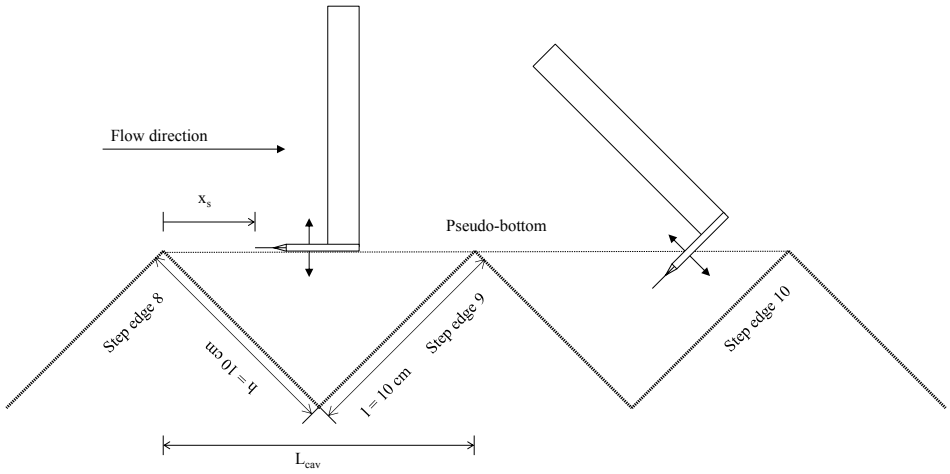

Figure 2. Probe alignment during air-water flow measurements

3. VOID FRACTION DISTRIBUTIONS

On a stepped chute, air is entrained because of interactions between the boundary layer outer edge and the free-surface (Rao and Rajaratnam 1961, Ervine and Falvey 1987, Chanson 1993, 2008). Figure 3 shows typical void fraction distributions at step edges for four dimensionless discharges (d_c/h = 0.9, 1.1, 1.3, 1.5), where y is the normal distance from the pseudo-bottom (y = 0), d_c is the critical depth, C is the time-averaged void fraction, x is the streamwise coordinate measured from the first step edge (Figure 1), x_i is the streamwise coordinate of the inception point, and L_{cav} is the step cavity length. All data followed an inverted S-shape distribution typically observed in skimming flows on stepped chutes with a variety of configurations (Chanson and Toombes 2002, Gonzalez and Chanson 2008, Bung 2009, Felder and Chanson 2011). The void fraction gradient ($\partial C/\partial y$) was maximum at about $C \approx 0.5$, indicating the largest level of air flux at that location (assuming that the gradient-diffusion hypothesis is valid). The void fraction profiles exhibited rapid longitudinal variations over the first 2-3 step edges downstream of the inception point as a result of flow bulking. Considering a control volume (CV) travelling downstream at a uniform velocity and neglecting any wall and buoyancy effects, its void fraction distribution is described by the 1-D diffusion equation:

$$\frac{\partial C}{\partial t} = D_t \frac{\partial^2 C}{\partial y^2} \tag{1}$$

where C is the void fraction, y is the normal distance from the pseudo-bottom (y = 0), and D_t is a turbulent diffusivity assumed to be independent of y. Assuming $D_t = D_t(t)$ so that the diffusivity is dependent of time, Equation (1) may be solved using the Laplace transform method with the following boundary condition:

$$C_{(y=Y_{50},t>0)} = 0.5 \tag{2}$$

where Y_{50} is the depth where C = 0.5. The solution is

$$C = \frac{1}{2} erfc\left(\frac{Y_{50} - y}{2\sqrt{\frac{D_a (x - x_i)}{V_a}}} \right) \tag{3}$$

where erfc is the complementary error function, V_a is the average streamwise velocity of the CV between x and x_i, and $D_a = \frac{1}{T}\int_0^{t=T} D_t dt$ (with $T = \frac{x - x_i}{V_a}$) is a time-averaged diffusivity. Note that for a steady and uniform flow with homogeneous turbulence, $D_a = D_t$. This solution is similar in form to that of a water jet discharging into the atmosphere (Chanson 1997, Brattberg et al. 1998). In Figure 3, Equation (3) is compared to the experimental data immediately downstream of the inception point (red curve). A good agreement was observed. It is noted that Equation (3) is unsuitable in regions where buoyancy or wall effects are important, particularly far downstream of the inception point of free-surface aeration.

Far downstream of the inception point, the flow became gradually varied, the void fraction profiles showed some self-similarity, and the effects of buoyancy must be accounted for. In this region, the conservation equation of air may be simplified into (Chanson 1995, 1997):

$$0 = \frac{\partial}{\partial y}\left(D_t \frac{\partial C}{\partial y} - u_{r,hyd} C \sqrt{1 - C} \cos\theta \right) \tag{4}$$

where $u_{r,hyd}$ is the bubble rise velocity in clear water with a hydrostatic pressure gradient and θ is the chute slope. Present data measured at the last step edge (step edge 12) were compared to a solution of Equation (4) obtained by Chanson and Toombes (2002):

$$C = 1 - \tanh^2\left(K - \frac{y / Y_{90}}{2D_0} + \frac{\left(y / Y_{90} - 1/3\right)^2}{3D_0}\right) \quad (5)$$

where Y_{90} is the depth where $C = 0.9$, K is an integration constant, and D_0 is a function of the depth-averaged void fraction $C_{mean} = \frac{1}{Y_{90}} \int_0^{Y_{90}} C dy$. Equation (5) generally compares well with the present data, despite some under-estimation for $y/d_c < 0.2 - 0.3$. This might be a result of vortical structures trapping bubbles in their centers and, hence, producing a local concentration of air-bubbles.

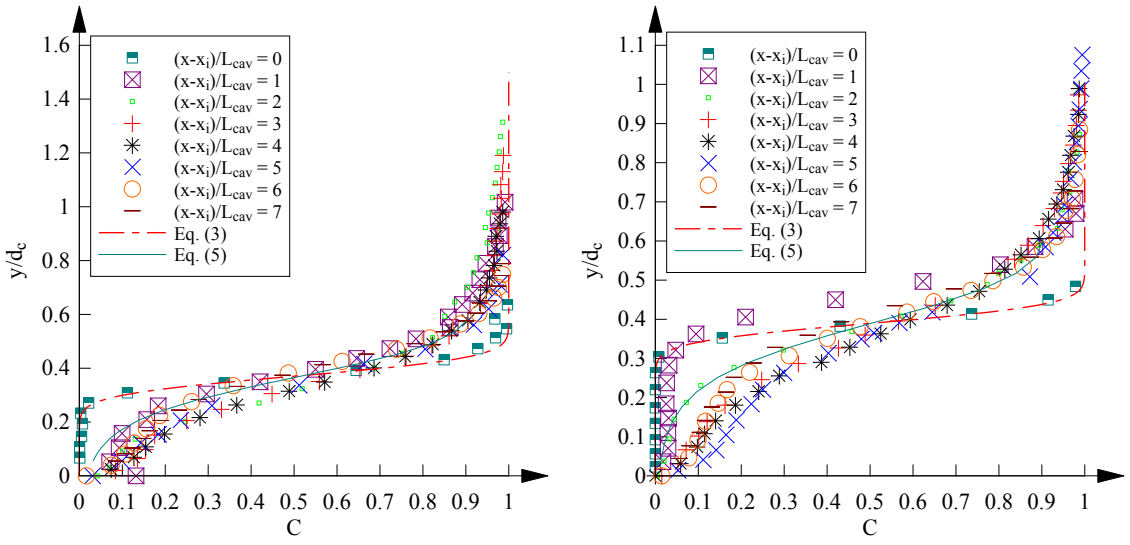

(A) $d_c/h = 0.9$ (B) $d_c/h = 1.1$

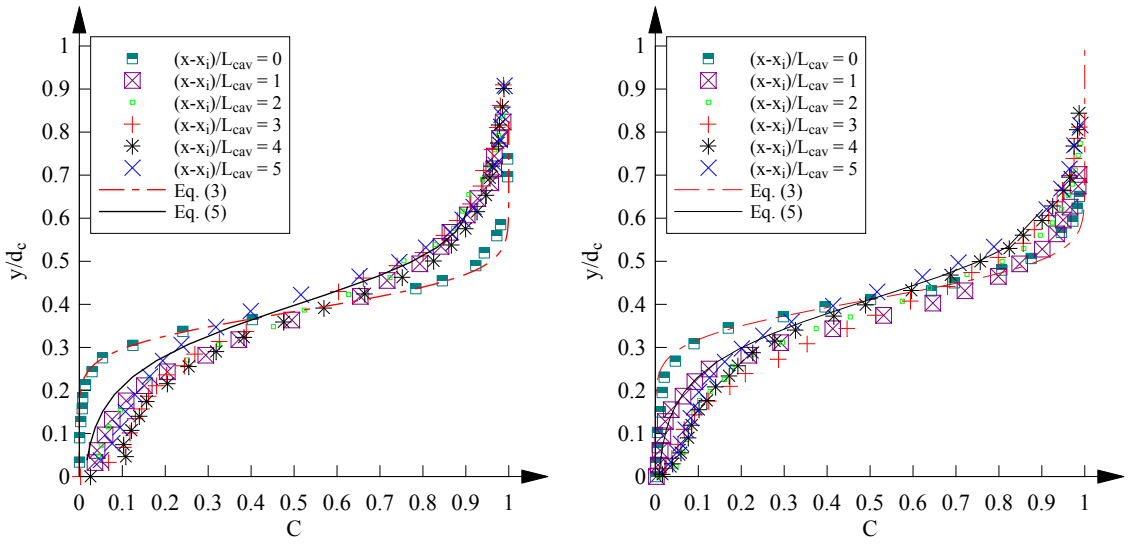

(C) $d_c/h = 1.3$ (D) $d_c/h = 1.5$

Figure 3. Void fraction distributions above step edges – Flow conditions: $\theta = 45°$, $h = 0.10$ m

Figure 4 shows the void fraction contours between step edges 7 and 9 for two skimming flow conditions (d_c/h = 0.9, 1.3), where x_s is the streamwise offset from step edge 8, and black symbols indicate measurement locations. For both discharges, the void fraction increased along the step cavity up to about 70% cavity length, then decreased towards the next step edge. This pattern might be a result of advective transport due to flow expansion and contraction over a step cavity. The recirculating cavity fluid trapped bubbles at its centre due to difference in air and water densities and is seen from the void fraction maxima found next to the cavity centres (Figure 4). This is especially evident for the larger discharge (Figure 4B).

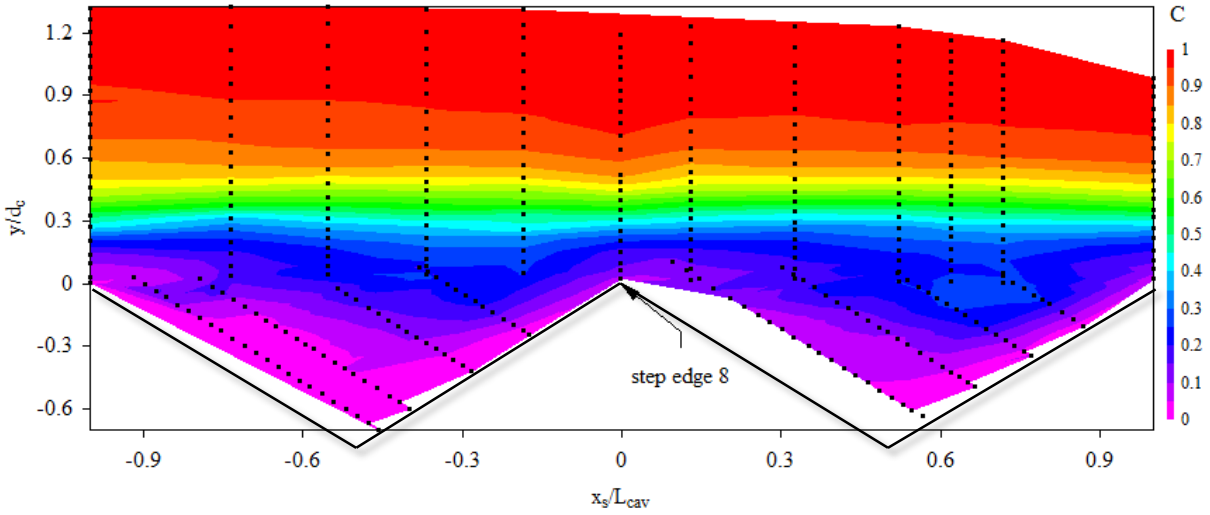

(A)

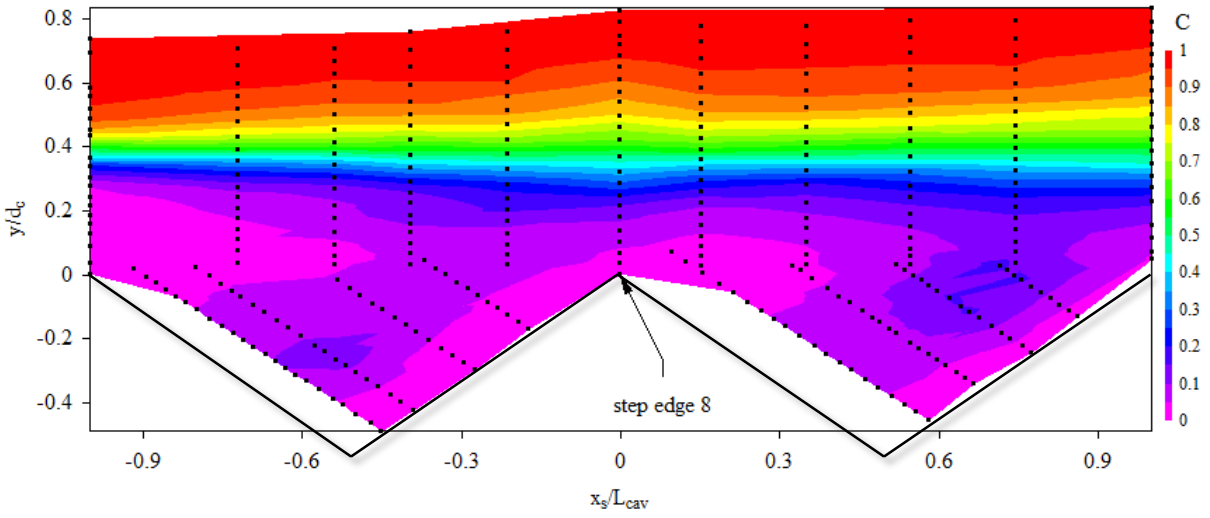

(B)

Figure 4. Void fraction contours between step edges 7 – 9 – Flow conditions: (A) d_c/h = 0.9, Re = 3.4×10^5; (B) d_c/h = 1.3, Re = 5.9×10^5; θ = 45°, h = 0.10 m – Step faces: solid black lines

4. BUBBLE COUNT RATE DISTRIBUTIONS

In stepped chute flows, the bubble count rate F is defined as half the number of air-water interfaces detected by the probe sensor per second and is proportional to the specific interfacial area (Chanson 2002). The dimensionless bubble count rate distributions at each step edge downstream of the inception point are plotted in Figure 5, where F is the bubble count rate and V_c is the critical velocity. All data approximately followed a bell-shape, with the largest bubble count rate observed at about $y/d_c = 0.3 - 0.4$ corresponding to a void fraction of about 0.5. This observation was consistent with several past studies (Chanson and Toombes 2002, Yasuda and Chanson 2003, Gonzalez and Chanson 2008). It may be reasoned that the bubble count rate should be proportional to the variance of the corresponding binary void fraction signal, which equals $C(1\text{-}C)$ and has a maximum at $C = 0.5$ (Chanson and Carosi 2007). Toombes (2002) demonstrated that the relationship between void fraction and bubble count rate may be approximated by:

$$\frac{F}{F_{max}} = 4C(1-C) \tag{6}$$

where F_{max} is the maximum bubble count rate at a cross-section. Equation (6) is compared to the present data in Figure 6, where the experimental data for $y < Y_{50}$ and $y \geq Y_{50}$ are shown in separate colors. Equation (6) was found to agree reasonably well with the present data for $y \geq Y_{50}$, but it differed significantly from those for $y < Y_{50}$. The non-linearly observed for $y < Y_{50}$ were likely induced by coherent fluctuations generated by the step edge, which implied that successive detections of air-water elements could not be assumed a random process. Away from the pseudo-bottom (i.e. $y \geq Y_{50}$), the effects of coherent structures became negligible and the assumptions for Equation (6) (see Toombes 2002) were more plausible. It is noted that these effects may be taken into account by a more advanced model proposed by Toombes and Chanson (2008).

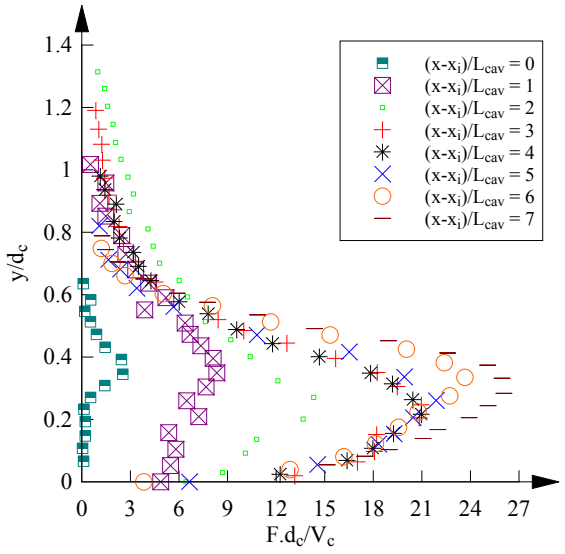

(A) $d_c/h = 0.9$

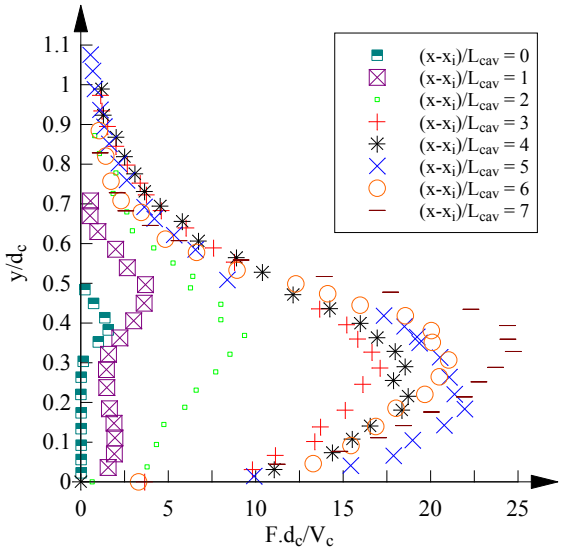

(B) $d_c/h = 1.1$

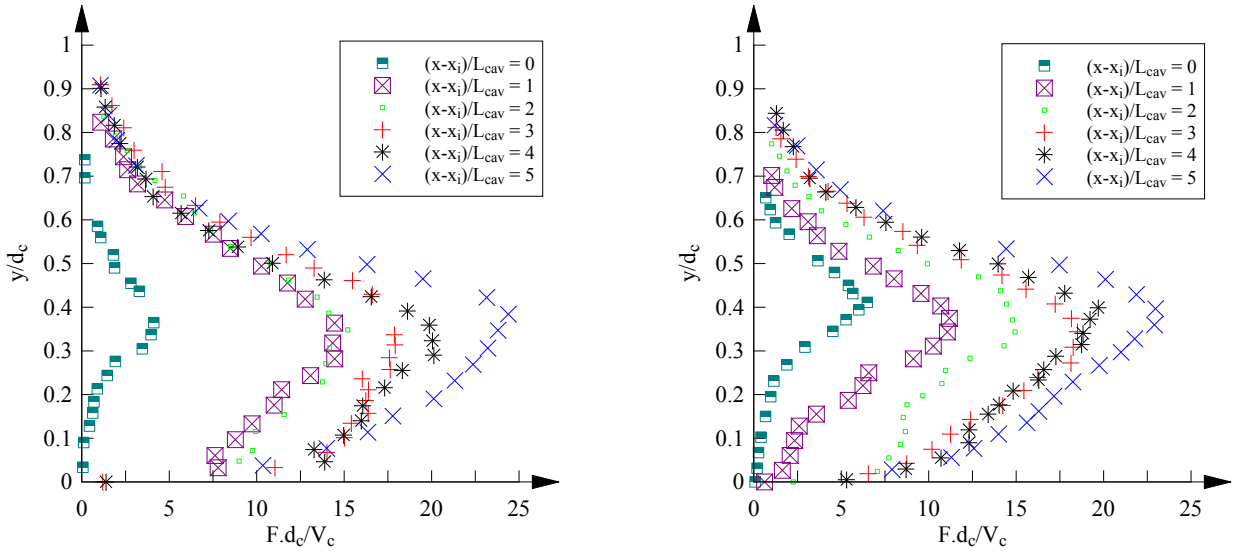

(C) $d_c/h = 1.3$ (D) $d_c/h = 1.5$

Figure 5. Bubble count rate distributions above step edges – Flow conditions: $\theta = 45°$, $h = 0.10$ m

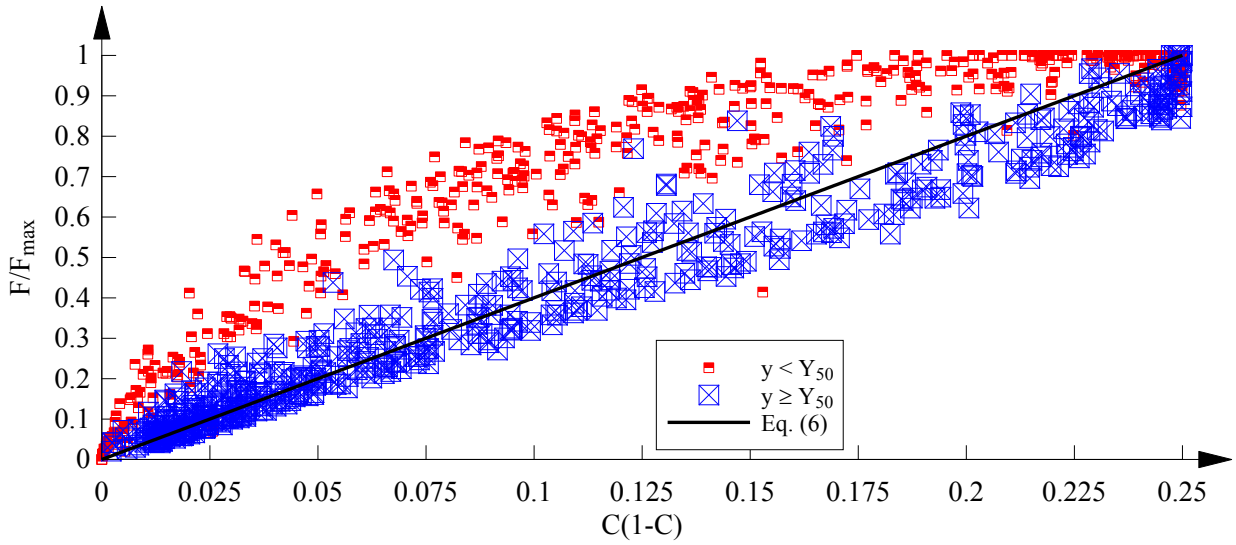

Figure 6. Relationship between void fraction and bubble count rate in skimming flows – Flow conditions: d_c/h = 0.9, 1.1, 1.3, 1.5, 1.7, $\theta = 45°$, $h = 0.10$ m

5. SELF-AERATION IN THE RAPIDLY-VARIED FLOW REGION

Immediately downstream of the inception point of aeration, turbulent transport is dominant over advective transport by the mean-flow and buoyancy. The new solution (Equation (3)) provides a satisfactory description of the diffusion process in this region. The flow depth variation in this region is a function of the depth averaged void fraction C_{mean}, which may be derived by integrating Equation (3) from 0 to Y_{90}. The lower limit of the integral may be replaced by $-Y_{90}$ using the method of images to account for any wall effects. The integration result yields:

$$C_{mean} = \frac{1.82\sqrt{\frac{D_a(x-x_i)}{V_a}}}{Y_{50} + 1.82\sqrt{\frac{D_a(x-x_i)}{V_a}}} \quad (7)$$

Figure 7 compares Equation (7) to the streamwise distributions of C_{mean}, where D_a and Y_{50} were derived from measured void fraction data. The agreement between Equation (7) and present data was generally good, including far downstream of the inception point (i.e. in the gradually-varied flow region). For the present data, the empirically determined apparent diffusivity D_a was best correlated with

$$\frac{D_a}{\sqrt{gd_c^3}} = 0.027 e^{-0.276\frac{x-x_i}{L_{cav}}} \quad (R = 0.876) \quad (8)$$

where R is the normalised correlation coefficient. The dimensionless form of Equation (8) (valid at step edges) suggested that it might be used in conjunction with Equation (7) in prototype applications when diffusivity data is not readily available. A further simplification may be made by letting $Y_{50} = d_i$ where d_i is the flow depth at the inception point (i.e. assuming the streamwise acceleration due to gravity is small). The simplification provides a practical means of estimating the flow bulking height in prototype structures.

A detailed examination of Figure 7 shows that C_{mean} typically increased rapidly immediately downstream of the inception point and reached a local maximum at about 2-4 cavity lengths downstream of the inception point of free-surface aeration, followed by a more gradual decrease. This de-aeration process was also observed by other authors (e.g. Matos 2000). It might occur when too much air was entrained initially. The turbulent diffusivity D_t may be derived by differentiating Equation (8):

$$\frac{D_t}{\sqrt{gd_c^3}} = 0.027\left(1 - 0.276\frac{x-x_i}{L_{cav}}\right) e^{-0.276\frac{x-x_i}{L_{cav}}} \quad (9)$$

Equation (9) is plotted in Figure 8. It is seen that, for the present data, the turbulent diffusivity increased to approximately 3.5 step lengths downstream of the inception point before becoming negative further downstream. Such a negative diffusivity implies a process of de-aeration, and its relation to C_{mean} becomes clear when Equation (1) is integrated from $-Y_{90}$ to Y_{90} (with the use of the method of images):

$$\frac{d}{dt}C_{mean} = \frac{D_t}{Y_{90}}\left(\frac{\partial C}{\partial y}_{y=Y_{90}} - \frac{\partial C}{\partial y}_{y=-Y_{90}}\right) \quad (10)$$

In skimming flows, the bracketed term can be shown to be positive by differentiating Equation (3) with respect to y (as long as the void fraction distribution is adequately described by Equation (3)). Thus, the total rate of change of the depth-averaged void fraction (dC_{mean}/dt) has the same sign as the diffusivity. Note that the present discussion is limited to a 1-D model neglecting any buoyancy effect. For completeness, some fragmented flow may experience a negative bracketed term: e.g., immediately downstream of a drop (Toombes and Chanson 2008).

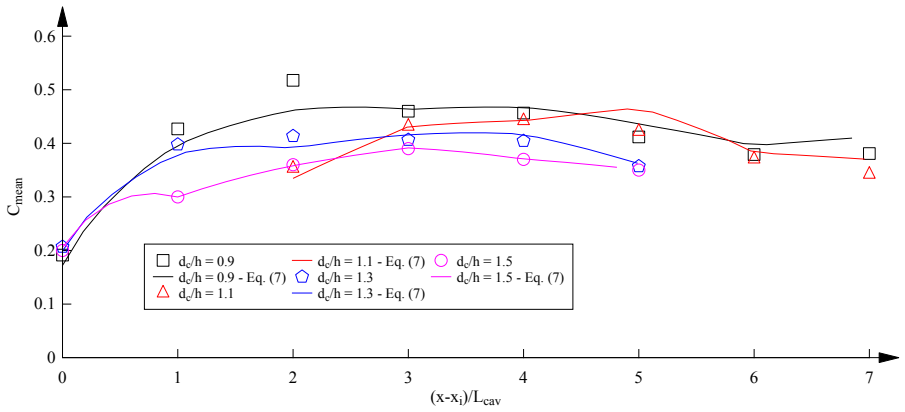

Figure 7. Steamwise distribution of depth averaged void fraction – comparison with Equation (7) – Flow conditions: $\theta = 45°$, $h = 0.10$ m

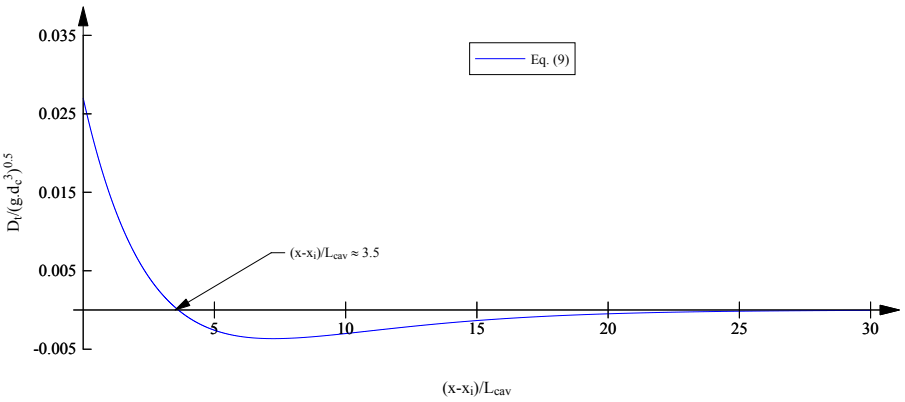

Figure 8. Streamwise distribution of turbulent diffusivity – Flow conditions: $\theta = 45°$, $h = 0.10$ m

6. CONCLUSION

On a stepped chute, self-aeration occurs when the turbulent boundary layer outer edge interacts with the free surface. A rapidly-varied flow region follows immediately downstream of the inception point of aeration. New void fraction distributions in this region were compared successfully to a newly proposed solution to the 1-D diffusion equation. Further downstream, the flow becomes gradually varied, and the experimental data were approximated closely by an existing solution of the steady state 1-D advection diffusion equation. Between step edges, the void fraction distributions showed variations consistent with flow expansion and contraction. The bubble count rate scaled with the void fraction signal variance, although their relationship was biased close to the wall under the influence of coherent motions. A simple model was proposed to describe the flow bulking in the rapidly-varied flow region and showed good agreement with the experimental data. It was found that flow bulking stopped at approximately 3.5 cavity lengths downstream of the inception point. The concept of negative diffusivity was introduced and was shown to be associated with flow de-aeration.

7. ACKNOWLEDGEMENTS

The authors acknowledge the technical assistance of Jason Van Der Gevel and Stewart Matthews (The University of Queensland). Some helpful input from Dr. Hang Wang (The University of Queensland) is acknowledged. The financial support of the Australian Research Council (Grant DP1201004841) is acknowledged.

8. REFERENCES

Brattberg, T., Chanson, H., and Toombes, L. (1998). Experimental investigations of free-surface aeration in the developing flow of two-dimensional water jets. *Journal of Fluids Engineering*, Transactions ASME, Vol. 120, No. 4, pp. 738-744 (DOI: 10.1115/1.2820731).

Bung, D.B. (2009). Zur selbstbelüfteten gerinnenströmung auf kaskaden mit gemässigter neigung. ('Self-aerated skimming flows on embankment stepped spillways.') *Ph.D. thesis*, University of Wuppertal, LuFG Wasserwirtschaft and Wasserbau, Germany, 292 pages (in German).

Chanson, H. (1993). Stepped spillway flows and air entrainment. *Canadian Journal of Civil Engineering*, Vol. 20, No. 3, June, pp. 422-435 (DOI: 10.1139/l93-057).

Chanson, H. (1994). Hydraulics of skimming flows over stepped channels and spillways. *Journal of Hydraulic Research*, Vol. 32, No. 3, pp. 445-460 (DOI: 10.1080/00221689409498745).

Chanson, H. (1995). Air bubble diffusion in supercritical open channel flow. *Proc. 12th Australasian Fluid Mechanics Conference,* AFMC, Sydney, Australia, R.W. Bilger Editor, Vol. 2, pp. 707-710.

Chanson, H. (1997). Air bubble entrainment in free-surface turbulent shear flows. Academic Press, London, UK, 401 pages (ISBN 0-12-168110-6).

Chanson, H. (2002). Air-water flow measurements with intrusive phase-detection probes. Can we improve their interpretation? *Journal of Hydraulic Engineering*, ASCE, Vol. 128, No. 3, pp. 252-255 (DOI: 10.1061/(ASCE)0733-9429(2002)128:3(252)).

Chanson, H. (2008). Advective diffusion of air bubbles in turbulent water flows. in Fluid Mechanics of Environmental Interfaces, Taylor & Francis, Leiden, The Netherlands, C. Gualtieri and D.T. Mihailovic Editors, Chapter 7, pp. 163-196.

Chanson, H., and Carosi, G. (2007). "Advanced post-processing and correlation analyses in high-velocity air-water flows." *Environmental Fluid Mechanics*, Vol. 7, No. 6, pp. 495-508 (DOI: 10.1007/s10652-007-9038-3).

Chanson, H., and Toombes, L. (2002). Air-Water flows down stepped chutes. Turbulence and flow structure observations. *International Journal of Multiphase Flow*, Vol. 28, No. 11, pp. 1737-1761 (DOI: 10.1016/s0301-9322(02)00089-7).

Ervine, D.A., and Falvey, H.T. (1987). Behaviour of turbulent water jets in the atmosphere and in plunge pools. *Proc. Institution of Civil Engineers*, Part 2, Mar., 83, pp. 295-314.

Felder, S., and Chanson, H. (2011). Air-water flow properties in step cavity down a stepped chute. *International Journal of Multiphase Flow*, Vol. 37, No. 7, pp. 732–745 (DOI: 10.1016/j.ijmultiphaseflow.2011.02.009).

Gonzalez, C.A., and Chanson, H. (2008). Turbulence manipulation in embankment stepped chute flows: an experimental study. *European Journal of Mechanics B/Fluids*, Vol. 27, No. 4, pp. 388-408 (DOI: 10.1016/j.euromechflu.2007.09.003).

Matos, J. (1999). Air entrainment and energy dissipation on stepped spillways. *Ph.D. thesis*, Technical University of Lisbon, Portugal.

Matos, J. (2000). Hydraulic design of stepped spillways over RCC dams. *Proc. The International Workshop on Hydraulics of Stepped Spillways*, Zürich, March 22-24, 2000, pp. 187-194.

Rao, N.S.G., and Rajaratnam, N. (1961). On the inception of air entrainment in open channel flows. *Proc. 9th IAHR Biennial Congress*, Dubrovnick, Yugoslavia, pp. 9-12.

Toombes, L. (2002). Experimental study of air-water flow properties on low-gradient stepped cascades. *Ph.D. Thesis*, Dept. of Civil Engineering, University of Queensland, Australia.

Toombes, L., and Chanson, H. (2008). Interfacial aeration and bubble count rate distributions in a supercritical flow past a backward-facing step. *International Journal of Multiphase Flow*, Vol. 34, No. 5, pp. 427-436 (DOI: 10.1016/j.ijmultiphaseflow.2005.01.005).

Wood, I.R., Ackers, P., Loveless, J. (1983). General method for critical point on spillways. *Journal of Hydraulic Engineering*, ASCE, 109, 308–312 (DOI: 10.1061/(asce)0733-9429(1983)109:2(308)).

Yasuda, Y., and Chanson, H. (2003). Micro- and macro-scopic study of two-phase flow on a stepped chute. *Proc. 30th IAHR Biennial Congress*, Thessaloniki, Greece, J. Ganoulis and P. Prinos Editors, Vol. D, pp. 695-702.